

Highly superporous cholesterol-modified poly(2-hydroxyethyl methacrylate) scaffolds for spinal cord injury repair

Šárka Kubinová,¹ Daniel Horák,^{2,3} Aleš Hejčík,^{1,4} Zdeněk Plichta,² Jiří Kotek,² Eva Syková^{1,3,5}

¹Institute of Experimental Medicine, Academy of Sciences of the Czech Republic, Vídeňská 1083, 14220 Prague 4, Czech Republic

²Institute of Macromolecular Chemistry, Academy of Sciences of the Czech Republic, Heyrovský Sq. 2, 16206 Prague 6, Czech Republic

³Center for Cell Therapy and Tissue Repair, Charles University, V Úvalu 84, 15006 Prague 5, Czech Republic

⁴Department of Neurosurgery, Masaryk Hospital, Sociální péče 3316/12a, 40011 Ústí nad Labem, Czech Republic

⁵Department of Neuroscience, 2nd Medical Faculty, Charles University, V Úvalu 84, 15006 Prague 5, Czech Republic

Received 14 February 2011; accepted 21 July 2011

Published online 27 September 2011 in Wiley Online Library (wileyonlinelibrary.com). DOI: 10.1002/jbm.a.33221

Abstract: Modifications of poly(2-hydroxyethyl methacrylate) (PHEMA) with cholesterol and the introduction of large pores have been developed to create highly superporous hydrogels that promote cell–surface interactions and that can serve as a permissive scaffold for spinal cord injury (SCI) treatment. Highly superporous cholesterol-modified PHEMA scaffolds have been prepared by the bulk radical copolymerization of 2-hydroxyethyl methacrylate (HEMA), cholesterol methacrylate (CHLMA), and ethylene dimethacrylate (EDMA) cross-linking agent in the presence of ammonium oxalate crystals to establish interconnected pores in the scaffold. Moreover, 2-[(methoxycarbonyl)methoxy]ethyl methacrylate (MCMEMA) was incorporated in the polymerization recipe and hydrolyzed, thus introducing carboxyl groups in the hydrogel to control its swelling and softness. The hydrogels supported

the *in vitro* adhesion and proliferation of rat mesenchymal stem cells. In an *in vivo* study of acute rat SCI, hydrogels were implanted to bridge a hemisection cavity. Histological evaluation was done 4 weeks after implantation and revealed the good incorporation of the implanted hydrogels into the surrounding tissue, the progressive infiltration of connective tissue and the ingrowth of neurofilaments, Schwann cells, and blood vessels into the hydrogel pores. The results show that highly superporous cholesterol-modified PHEMA hydrogels have bioadhesive properties and are able to bridge a spinal cord lesion. © 2011 Wiley Periodicals, Inc. *J Biomed Mater Res Part A*: 99A: 618–629, 2011.

Key Words: 2-hydroxyethyl methacrylate, scaffold, hydrogel, cholesterol, spinal cord repair, stem cells

How to cite this article: Kubinová Š, Horák D, Hejčík A, Plichta Z, Kotek J, Syková E. 2011. Highly superporous cholesterol-modified poly(2-hydroxyethyl methacrylate) scaffolds for spinal cord injury repair. *J Biomed Mater Res Part A* 2011;99A:618–629.

INTRODUCTION

Spinal cord injury (SCI) often results in permanent neurological deficits as a consequence of the inability of axons to regenerate across the lesion. Although the adult spinal cord is currently known to be capable of functional reorganization and axonal sprouting and, similarly as other regions of the adult central nervous system (CNS), the adult spinal cord contains neural stem and progenitor cells,¹ the inhibitory environment of the mature mammalian CNS, the glial scar barrier as well as cyst formation hinder neurons from regenerating across the site of injury.² Cell transplantation has emerged as a promising therapeutic approach for SCI.^{3,4} However, in the case of a large spinal cord lesion, when the cystic cavity is developed, cell transplantation alone is not

sufficient for tissue regeneration, and tissue repair requires “bridging” the lesion with a 3D permissive environment that can fill the tissue gap and concomitantly support axonal regeneration and the re-establishment of damaged connections.⁵

To develop appropriate materials, much of the current research is focused on both naturally derived and synthetic hydrogels due to their softness and flexibility,^{5,6} but also other materials, such as sponges, self-assembling nanofibers, tubes, and fibers, have been studied.^{7–12} Hydrogels are cross-linked hydrophilic polymers that swell in water, which can make their mechanical properties similar to those of the nervous tissue and concomitantly enable ion and metabolite exchange with tissue fluids. Naturally derived hydrogels comprising collagen,¹³ alginates,¹⁴ hyaluronic acid,^{15,16} agarose,¹⁷

Additional Supporting Information may be found in the online version of this article.

Correspondence to: Š. Kubinová; e-mail: sarka.k@biomed.cas.cz

Contract grant sponsor: Czech Science Foundation; contract grant numbers: P304/11/0731, P304/11/P633, 108/10/1560, P304/11/0653

Contract grant sponsor: Academy of Sciences of the Czech Republic; contract grant numbers: KAN200520804, IAA50039092

Contract grant sponsor: Ministry of Education, Youth and Sports of the Czech republic; contract grant number: 1M0538

or fibrin¹⁸ have been reported to be promising scaffolding materials for the treatment of SCI as they are nontoxic, biocompatible, and mostly biodegradable.¹⁹ The synthetic hydrogels used for spinal cord implantation include poly(ethylene glycol),²⁰ poly(2-hydroxyethyl methacrylate) (PHEMA),^{21–23} or poly[N-(2-hydroxypropyl) methacrylamide] (PHPMA).^{22,24}

For neural repair, hydrogels are additionally being designed for cell transfer^{12,25} or as carriers for the sustained local delivery of chondroitinase,²⁶ neurotrophic factors,²⁷ or other drugs and bioactive substances.²⁸

PHEMA has been widely used as a biomaterial due to its good biocompatibility and the possibility to tailor its physical and chemical properties.²⁹ Since PHEMA does not have cell-adhesive properties, additional modification of this polymer is needed to promote cell-surface interactions. To improve the bioactivity of PHEMA scaffolds, the introduction of groups with positive charges³⁰ or modification with laminin-derived peptides have been previously employed.^{31,32} In a previous report, we have demonstrated that cholesterol-modified superporous PHEMA scaffolds (with a pore size from 10^1 to 10^2 μm) display significantly improved bioadhesive properties and support cell adhesion and proliferation.³³ However, the elastic modulus of these scaffolds, ~ 130 kPa, was much higher than the elastic modulus determined for neuronal tissue, ~ 1 –4 kPa,^{34,35} and therefore not suitable for application in neural tissue engineering, especially for spinal cord treatment. In the present study, we aimed to increase the swellability and softness of cholesterol-modified PHEMA hydrogels and to design highly superporous scaffolds possessing good mechanical properties that could be utilized as implants in the soft spinal cord tissue. In contrast to superporous scaffolds with $\sim 45\%$ inorganic porogen loading, highly superporous hydrogels possess more porogen, amounting to 60–65% of the entire hydrogel volume. Novel cholesterol-modified superporous PHEMA scaffolds have been prepared by the bulk radical copolymerization of 2-hydroxyethyl methacrylate (HEMA), cholesterol methacrylate (CHLMA), and the crosslinking agent ethylene dimethacrylate (EDMA) in the presence of ammonium oxalate crystals to introduce interconnected superpores in the matrix. To increase swellability, an additional monomer, 2-[(methoxycarbonyl)methoxy]ethyl methacrylate (MCMEMA), was incorporated in the polymerization recipe and hydrolyzed to [2-(methacryloyloxy)ethoxy]acetic acid (MOEAA), thus introducing carboxyl groups in the polymer. Three types of PHEMA hydrogels containing 2 wt %, 4 wt %, and 8 wt % of MOEAA were prepared, differing both in swelling and charge.

To evaluate the *in vitro* biocompatibility of the hydrogels, cell adhesion and proliferation were studied using mesenchymal stem cells (MSCs). MSCs have been increasingly used in cell therapy and tissue engineering, due to their regenerative potential and capacity to differentiate into various cell types after implantation into injured tissue.³⁶ Moreover, it has been shown recently that PHPMA hydrogels seeded with MSCs and implanted into a chronic spinal cord lesion prevented tissue atrophy and improved behavioral

outcome.³⁷ To determine their ability to bridge a spinal cord lesion, the hydrogels were implanted into an acute model of SCI in rats (hemisection), and their regenerative potential was histologically evaluated 4 weeks after implantation.

MATERIALS AND METHODS

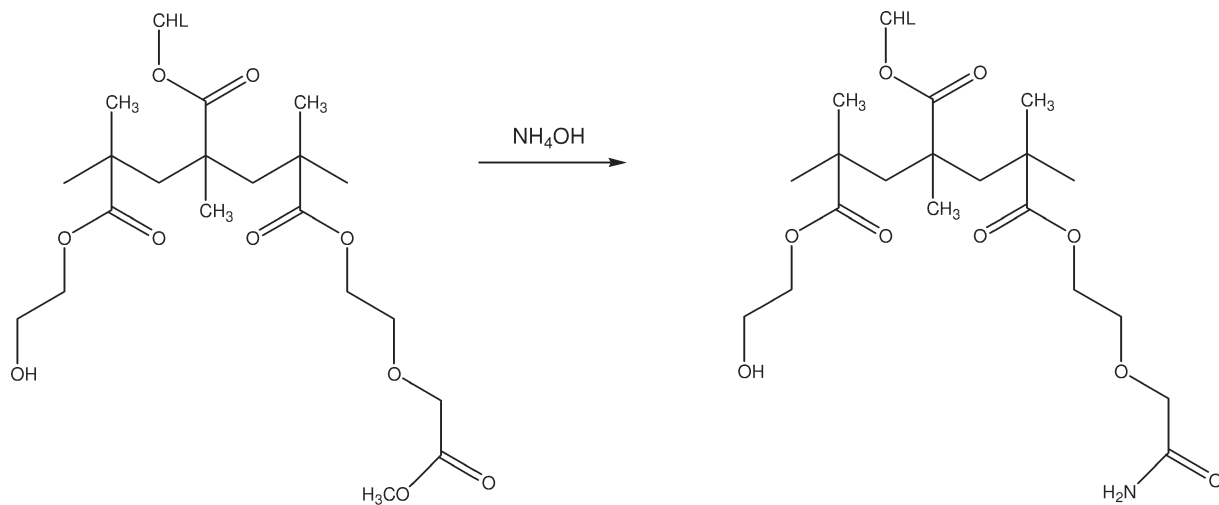
Reagents

HEMA (Röhm, Germany) and EDMA (Ugilor S.A., France) were distilled under reduced pressure. MCMEMA and CHLMA were synthesized according to a previously published procedure.³³ 2,2'-Azobisisobutyronitrile (AIBN) was obtained from Fluka, Buchs, Switzerland. Ammonium oxalate (Lachema, Brno, Czech Republic) was crystallized from water under the formation of 30–90 μm thick and about 0.3–10 mm long needle-like crystals and used as a porogen. All other chemicals were obtained from Sigma-Aldrich (St. Luis, MO).

Dulbecco's modified Eagle's medium (DMEM) and fetal bovine serum (FBS), purchased from PAA Laboratories (Pasching, Austria), and Primocin™ purchased from Lonza (Cologne, Germany) were used for cell cultivation. The WST-1 assay was purchased from Roche (Mannheim, Germany). Ampicillin, atropine, and mesocain were purchased from BB Pharma (Prague, Czech Republic). For immunofluorescent staining, Chemiblocker, Triton X-100, bovine serum albumin (BSA), mouse anti-vinculin, Cy3-conjugated mouse anti-GFAP, mouse anti-NF 160 and mouse anti-NF 200 purchased from Sigma-Aldrich, rabbit anti-NGF Receptor p75 purchased from Millipore (Temecula, CA), mouse anti-RECA-1 purchased from Abcam (Cambridge, MA), Alexa-Fluor 568 phalloidin, 4',6-diamidino-2-phenylindole (DAPI), and goat anti-mouse IgG conjugated with Alexa-Fluor 488 or Alexa-Fluor 594, purchased from Molecular Probes (Invitrogen, Paisley, UK), were used.

Preparation of superporous P(HEMA-CHLMA) hydrogel implants

In a typical experiment, a 5 mL polyethylene syringe equipped with a stainless 32- μm mesh was loaded in a dust-free box with a suspension of freshly crystallized ammonium oxalate (2.55 g; 42.3 vol %) in water. The excess solution was removed by centrifugation, and the crystals washed with ethanol and dried at room temperature. The hot (90°C) saturated solution (3 mL) of ammonium oxalate was again loaded and additional crystals were precipitated after cooling. This procedure was repeated three times. The monomer mixture, including HEMA (2.375 or 2.225 g), MCMEMA (50 or 200 mg; 2 or 8 wt %), CHLMA (50 mg; 2 wt %), EDMA (25 mg; 1 wt %), AIBN (10 mg), and 1,4-dioxane (1.25 mL), was then added and the syringe sealed. The mixture was polymerized at 60°C for 16 h; the syringe was then cut lengthwise and the hydrogel cylinder removed. The resulting superporous poly(2-hydroxyethyl methacrylate-co-2-[(methoxycarbonyl)methoxy]ethyl methacrylate-co-cholesterol methacrylate-co-ethylene dimethacrylate) [P(HEMA-MCMEMA-CHLMA-EDMA)], in the text further abbreviated as P(HEMA-CHLMA)], cylinder was incubated at room



SCHEME 1. Ammonolysis of P(HEMA-MCMEMA) hydrogel.

temperature first in a saturated solution of NaCl for 24 h (to avoid cracks) and then in 300 mL of 0.025M H₂SO₄ for 24 h to hydrolyze the MCMEMA moiety, yielding MOEAA. This was followed by repeated washing with water (200 mL each time) for 4 days, treatment at 23°C with 300 mL of 0.05M NaOH for 6 h, and finally by washing with water until a neutral pH was reached.

Analogously, the P(HEMA-MCMEMA-CHLMA-EDMA) cylinder was washed in a saturated solution of NaCl and water for 4 h, followed by washing with 5% ammonium hydroxide solution at 45°C for 16 h to transform MCMEMA into 2-(2-amino-2-oxoethoxy)ethyl methacrylate (AOEEMA) (Scheme 1). Finally, the cylinder was washed with water, 0.05M HCl, and water. For the cell culture experiments, cylinders were cut into 0.7-mm thick discs using an HM650V Vibroslicer (Microm, Walldorf, Germany), washed with water, 0.025M H₂SO₄, 0.1M NaOH, and water, and finally sterilized in an autoclave for 30 min at 120°C.

Hydrogel characterization

Scanning electron microscopy (SEM) images were acquired using a JSM 6400 (Jeol, Tokyo, Japan) scanning electron microscope. The samples were sputter-coated with 4 nm of Pt before imaging. Fluorescent images were acquired by a LSM DUO5 laser scanning confocal microscope (Zeiss, Jena, Germany).

Swelling (S_w) and water regain in pores (P) were estimated by weighing water-soaked PHEMA cylinders before (m_w) and after centrifugation (m_c) (800g). Hydrogels were swollen in water for at least 16 h. Water regain in pores was determined as $P = (m_w - m_c)/m_c$ (g/g). Swelling was defined as $S_w = (m_c - m_o)/m_o$ (g/g), where m_o is the weight of the dried polymer.

Mechanical testing

The stiffness of highly superporous P(HEMA-2%MOEAA-CHLMA), P(HEMA-8%MOEAA-CHLMA), and P(HEMA-4%MOEAA-4%AOEEMA-CHLMA) samples was assessed by compressive testing. Cylindrical specimens having an h/D

(height-to-diameter) ratio equal to 1 were exposed to a compressive load using an Instron 5800R (Norwood, MA) universal tester. The diameter of the cylinders was approximately 12.5 mm. The tests were performed at a constant speed of 0.5 mm/min at ambient temperature. During the test the cylinders were immersed in a phosphate buffer. From the initial straight-line portion of the stress-strain diagram, a modulus of elasticity was calculated by dividing the change in stress $\sigma_2 - \sigma_1$ by the corresponding change in strain $\varepsilon_2 = 0.10$ minus $\varepsilon_1 = 0.05$. Assessment of the modulus is schematically depicted in Figure 1.

Cell culture

MSCs were isolated from 4-week-old Wistar rats. The bone marrow was extruded from the femurs using a needle and a syringe with MSC culture medium containing DMEM with 10% FBS and Primocin™ (100 µg/mL). After 24 h, the non-adherent cells were removed by replacing the medium. Cultures were kept in a humidified 5% CO₂ atmosphere at 37°C; cells up to the third passage were used for seeding hydrogel discs. Sterile hydrogel discs were placed into a 24-well plate with MSC culture medium, seeded with a suspension of 40,000 cells per disc and incubated for 1–5 days. Cell viability was determined by the WST-1 assay based on the spectrophotometric quantification of the water-soluble formazan dye. One, three and five days after seeding, the discs were washed with culture medium and placed into a new well with 0.5 mL culture medium. Fifty microliters of the WST-1 reagent were added to each disc, and the discs were incubated for 3 h at 37°C to form formazan. Two hundred microliters of formazan-containing medium were then transferred from each well to a 96-well plate. The absorbance was measured using a Tecan Spectra ELISA plate reader (Tecan Trading, Männedorf, Switzerland) at a wavelength of 450 nm.

The morphology of the cells grown on the hydrogels was examined by immunofluorescent staining for actin filaments and vinculin. After fixation in paraformaldehyde in PBS for 15 min, the cells were washed with 0.1M PBS and

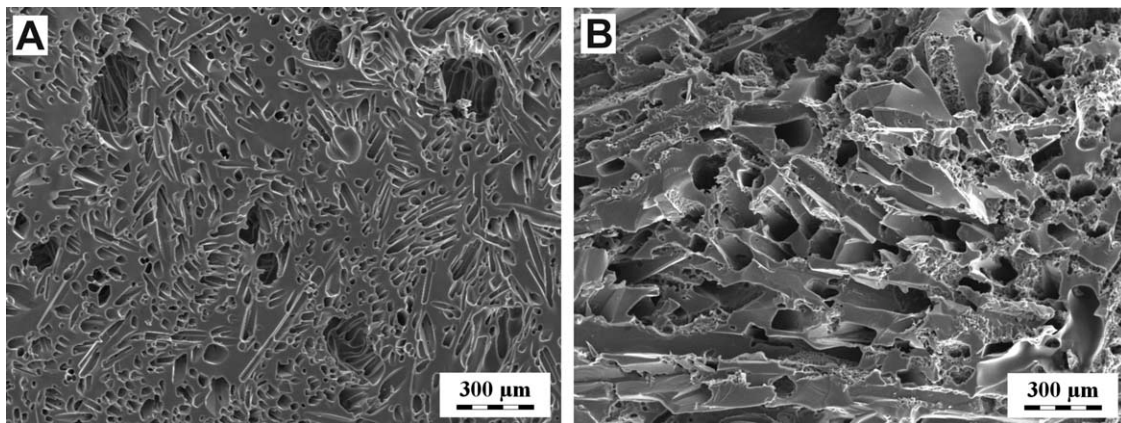


FIGURE 1. SEM micrograph of cross-sections of (A) conventional superporous and (B) highly superporous P(HEMA-2%MOEAA-CHLMA) hydrogels.

treated with Chemiblocker (1:20) and Triton X-100 (0.5%) in PBS. MSCs were incubated with Alexa-Fluor 568 phalloidin (1:300) and with an antibody directed against vinculin (1:200) diluted in 0.1M PBS containing 1% BSA and Triton X-100 (0.5 wt % solution). This was followed by incubation with a secondary goat anti-mouse IgG antibody conjugated with Alexa-Fluor 488 (1:200) diluted in 0.1M PBS containing Triton X-100 (0.5 wt %). After washing with PBS, the nuclei were visualized by using 4',6-diamidino-2-phenylindole (DAPI) fluorescent dye.

Hydrogel implantation

Twelve male rats (Wistar Velaz, Czech Republic) with a weight of 250–300 g underwent a hemisection at the level of the 8th thoracic vertebra (Th8). The animals were intraperitoneally injected with pentobarbital for anesthesia (solution of 1 g/100 mL, 6 mL/kg of animal weight); one dose of ATB (ampicillin 0.3 mL s.c.), atropine (0.2 mL s.c., 1:5), and mesocain to enhance local anesthesia (0.3 mL s.c. and i.m.) was administered preoperatively. A linear skin incision was performed above the spinous processes of Th7–9; the paravertebral muscles were detached from the laminae Th7–9, and a Th8 laminectomy was performed. The dura was incised, and about 2 mm × 2 mm × 2 mm of spinal cord tissue was dissected to form a hemisection cavity on the right side of the spinal cord. The animals were divided into three groups and P(HEMA-2%MOEAA-CHLMA), P(HEMA-4%MOEAA-4%-AOEEMA-CHLMA), or P(HEMA-8%MOEAA-CHLMA) sterile hydrogels were properly trimmed to adjust to the size and shape of the cavity. The hydrogel was implanted in such a way as to ensure that it would firmly adhere to the edges of the hemisection cavity without causing any undue pressure on the surrounding spinal cord tissue. The dura mater was sutured with a 10/0 monofil unresorbable thread (B Braun, Aesculap, Melsungen, Germany). The muscles and skin were sutured with a 4/0 monofil unresorbable thread (4/0 Chirmax, Prague, Czech Republic), and the animals were housed two in a cage with food and water *ad libitum*. The study was performed in accordance with the European Communities Council Directive of November 24, 1986 (86/609/EEC)

regarding the use of animals in research and was approved by the Central Commission for Animal Protection of the Academy of Sciences of the Czech Republic in Prague.

Tissue processing and histology

Four weeks after the hydrogel implantation, the animals were deeply anesthetized with an intraperitoneal injection of overdose pentobarbital and perfused with physiological saline followed by 4% paraformaldahyde in 0.1M phosphate buffer. The spinal cord was left in bone overnight, then removed and postfixed in the same fixative for at least 1 week. A 3-cm long segment of the spinal cord containing the lesioned site was dissected out, and a series of 40 μm thick longitudinal sections was collected. Hematoxylin-eosin (H&E) staining was performed using a standard protocol. For immunohistological testing, antibodies directed against the following markers were used: GFAP (1:200) to identify astrocytes, NF 160 and NF 200 (1:200) to identify neurofilaments, p75 (1:100) to identify Schwann cells, and RECA-1 (1:50) to identify endothelial cells of blood vessels. Alexa Fluor 488-conjugated goat anti-rabbit IgG (1:200) and Alexa Fluor 594-conjugated goat anti-rabbit IgG (1:500) were used as secondary antibodies. The nuclei were visualized by using 4',6-diamidino-2-phenylindole (DAPI) fluorescent dye.

Quantification of the neurofilament infiltration into the hydrogel

Longitudinal histological sections were collected, and every fifth section from each type of implanted hydrogel was immunostained for NF 160. The sections were examined with a fluorescent camera (Zeiss) and photographed using AxioVs40V Axiovision software (Zeiss). The area of neurofilaments (NF) that infiltrated the hydrogel was delineated in each section, and the area of NF infiltration was calculated as (area of NF/area of hydrogel in the section) × 100.

Statistical analysis

The values were calculated as mean ± standard deviations. Statistically significant differences ($p < 0.05$) were determined using a one-way ANOVA test.

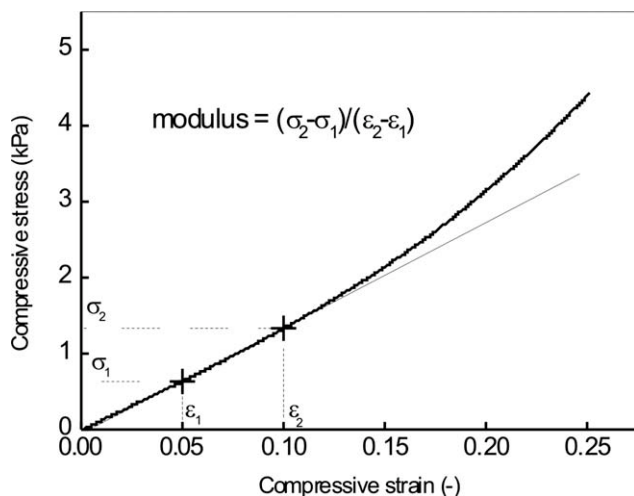


FIGURE 2. Schematic illustration of elasticity modulus assessment. Typical stress-strain curve for P(HEMA-2%MOEAA-CHLMA) hydrogel.

RESULTS AND DISCUSSION

Fabrication of highly superporous cholesterol-modified PHEMA scaffolds

Cellular adhesion to implants is important as it mediates many aspects of biocompatibility. The modification of PHEMA hydrogels with a functional group is necessary for *in vitro* cellular adhesion as well as for *in vivo* tissue infiltration when a hydrogel is implanted into neuronal tissue. Surface charge is considered to be one of the factors influencing tissue ingrowth into an implanted hydrogel.^{30,38,39} To facilitate cell adhesion on a polymer matrix, cholesterol-modified PHEMA hydrogels (2 wt % CHLMA) were designed and proved to be successful for tissue engineering applications.³³ The polymer matrix, however, has to contain reactive functional groups if immobilization of biomolecules is required. Therefore, an additional monomer, MCMEMA, was incorporated in the polymerization recipe, which was hydrolyzed to MOEAA after the completion of polymerization, thus introducing carboxyl groups in the polymer (Scheme 1) to control swellability and softness and to facilitate the subsequent attachment of adhesive peptides, antibodies, or other biomolecules. Moreover, EDMA (1 wt %) was also used as a crosslinking agent comonomer, thus hindering the dissolution of the resulting material in biological fluids. The presence of CHLMA in the PHEMA hydrogel is then important to improve the cell adhesion.³³

To repair an SCI by implanting a polymer scaffold, it is important that the implant's porosity and softness are comparable to those of the nervous tissue. If the hydrogel is too

stiff, the mismatch in mechanical properties between the native tissue of the soft spinal cord and the implant may result in the failure of the implant. Moreover, cysts between the implant and the surrounding spinal cord tissue might be formed after implantation (Supporting Information Fig. 1).

The porosity (macro-, micro-, and nanopores) of the hydrogel scaffold plays an important role in enabling cell attachment and migration, as well as the diffusion of nutrients. Moreover, the substrate's elasticity has been shown to regulate the differentiation of MSCs into a neuronal phenotype³⁴ as well as neurite outgrowth.⁴⁰

To increase the pore volume, the syringe used as a mold for the fabrication of the P(HEMA-CHLMA) scaffolds was repeatedly (three times) charged with ammonium oxalate crystals. The procedure used for the preparation of the scaffold, namely the repeated addition of a hot saturated ammonium oxalate solution to previously introduced crystals, has been described in the Experimental section. Three highly superporous scaffolds were designed: (i) P(HEMA-2%MOEAA-CHLMA), (ii) P(HEMA-4%MOEAA-4%AOEEMA-CHLMA), and (iii) P(HEMA-8%MOEAA-CHLMA). As a result of repeated ammonium oxalate loading, the content of the crystals in the hydrogel increased to 65 vol %. The crystals in the polymer matrix maintained their diameter and length up to several millimeters. After washing-out of the salt, 30–100 μm pores were then imprinted in the conventional superporous PHEMA matrices (Fig. 2). Such pore size is desirable for the ingrowth of cells into the scaffold matrix.

More pores with thinner walls were seen in highly superporous P(HEMA-2%MOEAA-CHLMA) hydrogel [Fig. 1(B)], in which faster diffusion of low-molecular-weight compounds can be expected, than in conventional superporous P(HEMA-2%MOEAA-CHLMA) hydrogel filled with a porogen only once [Fig. 1(A)].

To increase the hydrophilicity, highly superporous P(HEMA-8%MOEAA-CHLMA) hydrogel was prepared with a fourfold greater amount of MOEAA moiety than in the P(HEMA-2%MOEAA-CHLMA) scaffold. As a consequence, the former hydrogel swelled in water about 2.7 times more compared with the latter one (Table I). Superporous P(HEMA-MOEAA-CHLMA) hydrogels (typical $S_w > 1$ g water/g dry polymer) swelled more than neat PHEMA, which contained only 0.38 g water/g of dry hydrogel. In order that the hydrophilic scaffolds were not only highly swellable, but at the same time also contained a limited amount of acids (MOEAA), which could be a limiting factor in biological tests (acid possibly irritating the tissue), highly superporous P(HEMA-8%MCMEMA-CHLMA) hydrogel was modified by a reaction with ammonium hydroxide. This resulted in about

TABLE I. Physico-Chemical Properties of Highly Superporous Cholesterol-Modified PHEMA Hydrogels

| | Oxalate Content (mL/mL of feed) | S_w (g/g) | P (g/g) | N (wt %) | E (kPa) |
|--------------------------------|------------------------------------|-------------|---------|----------|--------------|
| P(HEMA-2%MOEAA-CHLMA) | 1.44 | 0.93 | 1.49 | – | 16.72 ± 5.34 |
| P(HEMA-4%MOEAA-4%AOEEMA-CHLMA) | 1.44 | 1.31 | 1.06 | 0.3 | 19.05 ± 3.69 |
| P(HEMA-8%MOEAA-CHLMA) | 1.44 | 2.50 | 1.74 | – | 10.06 ± 1.76 |

S_w , swelling; P, water regain in pores; N, nitrogen content; E, elastic modulus.

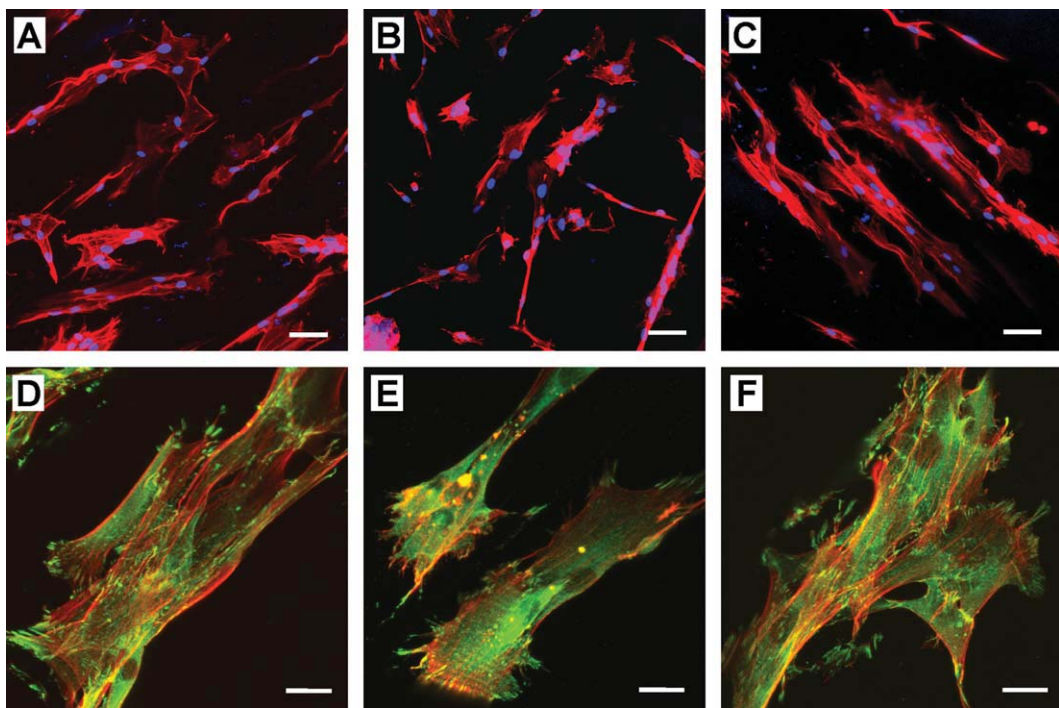


FIGURE 3. Laser scanning confocal micrographs of immunofluorescent staining for phalloidin (red) and cell nuclei (DAPI, blue) (A–C) and for phalloidin (red) and vinculin (green) (D–F) in MSCs seeded on highly superporous (A, D) P(HEMA-2%MOEAA-CHLMA), (B, E) P(HEMA-4%MOEAA-4%AOEEMA-CHLMA), and (C, F) P(HEMA-8%MOEAA-CHLMA) hydrogels for 2 days. MSCs spread mostly into the pores of the hydrogels. Scale bar: (A–C) 50 μ m, (D–F) 10 μ m. [Color figure can be viewed in the online issue, which is available at wileyonlinelibrary.com.]

50% ammonolysis of MCMEMA to 2-(2-amino-2-oxoethoxy)-ethyl methacrylate (AOEEMA) as confirmed by nitrogen analysis (Table I). The advantage of highly superporous P(HEMA-4%MOEAA-4%AOEEMA-CHLMA) hydrogel consists in the fact that its swelling is not so strongly pH-dependent, in contrast to P(HEMA-8%MOEAA-CHLMA) hydrogel. So, for example, while the volume of a highly superporous P(HEMA-8%MOEAA-CHLMA) cylinder was 2.2 mL at pH 2, it was 4.8 mL at pH 12. In contrast, the volume of a highly superporous P(HEMA-4%MOEAA-4%AOEEMA-CHLMA) cylinder was 4 mL at pH 2 and 4.6 mL at pH 12. With an increasing content of carboxyl groups (MOEAA) in highly superporous hydrogels, not only their swelling in water but also their pore volume increased (Table I). However, both values decreased after partial ammonolysis, probably due to a lower content of carboxyl groups.

Water regain in pores (P) should roughly correspond to the content of ammonium oxalate in the polymerization feed (Table I). The differences in the pore volume from the amount of porogen added in the feed in highly superporous P(HEMA-8%MOEAA-CHLMA) and P(HEMA-4%MOEAA-4%AOEEMA-CHLMA) hydrogels can be ascribed to inaccurate measurements due to the difficulty of manipulating a very soft (mechanically unstable) material (Table I). Nevertheless, highly superporous cholesterol-modified PHEMA hydrogels had a sufficient size and pore volume to accommodate cells. As the pore walls were intentionally weakened, the scaffolds contained a minimum amount of the polymer, which resulted in its softness.

To correlate the compliance of the hydrogels with the results of biomedical experiments, the modulus of elasticity of highly superporous P(HEMA-2%MOEAA-CHLMA), P(HEMA-4%MOEAA-4%AOEEMA-CHLMA), and P(HEMA-8%MOEAA-CHLMA) cylinders was measured (Fig. 2). The results obtained from compressive tests are summarized in Table I. As the modulus is a measure of stiffness, which is a reciprocal characteristic to compliance, it can be seen that the most compliant is P(HEMA-8%MOEAA-CHLMA). On the other hand, P(HEMA-4%MOEAA-4%AOEEMA-CHLMA) is rather rigid, exhibiting the highest modulus value, while P(HEMA-2%MOEAA-CHLMA) has a moderate stiffness. Conventional superporous cholesterol-modified PHEMA hydrogels described previously⁴¹ exhibit an elastic modulus of 134.9 ± 19.4 kPa. It is obvious that the moduli of highly superporous P(HEMA-MOEAA-CHLMA) scaffolds are lower by an order of magnitude and, therefore, that the superporous scaffolds are much more suitable for neural tissue applications.

In vitro cell growth

Morphological observation of attached MSCs seeded on highly superporous cholesterol-modified PHEMA hydrogels was done after 3 days of culture using immunofluorescent staining for F-actin and vinculin (Fig. 3). Cells attached and spread mostly in the pores of all hydrogels and formed well developed parallel organized microfilaments [Fig. 3(A–F)] as well as vinculin adhesion spots [Fig. 3(D–F)]. These findings correspond with our previous results on superporous cholesterol-modified PHEMA hydrogels³³ and confirm the

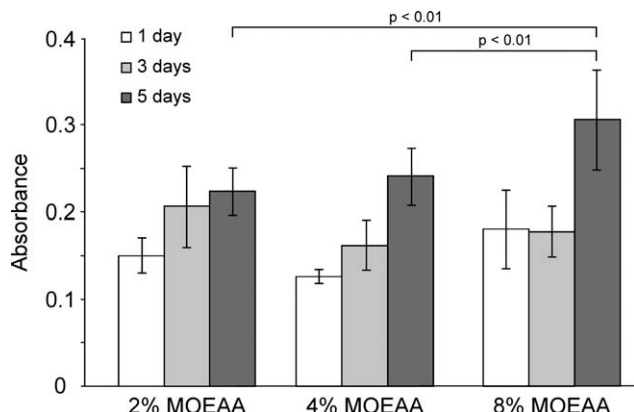


FIGURE 4. The viability of MSCs seeded on highly superporous PHEMA hydrogels (mean \pm S.D., $n = 6$).

bioadhesive role of the cholesterol modification. In our prior work, we demonstrated that cells also attach to neat superporous PHEMA hydrogels, but do not spread and remain in a spherical shape. We have also reported that serum proteins proved to be necessary for cell spreading on the surface of superporous cholesterol-modified PHEMA hydrogels.³³

Cell viability on the hydrogels was investigated after 1, 3, and 5 days of culture (Fig. 4) and revealed that all the highly superporous cholesterol-modified PHEMA hydrogels are non-cytotoxic and support cell proliferation. The fact that no significant differences in cell viability were found among the different types of hydrogel after 1 day suggests that the hydrogels have similar cell adhesive properties. Significantly higher cell viability was subsequently found for P(HEMA-8%MOEAA-CHLMA) hydrogels vs. P(HEMA-2%MOEAA-CHLMA) ($p < 0.01$) as well as vs. P(HEMA-4%MOEAA-4%AOEEMA-CHLMA) ($p < 0.01$) after 5 days. This suggests that the higher porosity and at the same time higher compliance (lower modulus of elasticity) of the P(HEMA-8%MOEAA-CHLMA) hydrogels might promote cell migration, growth, and proliferation.

Histological evaluation of hydrogels implanted into SCI

Highly superporous P(HEMA-2%MOEAA-CHLMA), P(HEMA-4%MOEAA-4%AOEEMA-CHLMA), and P(HEMA-8%MOEAA-CHLMA) hydrogels were implanted into hemisected spinal cords, and the biocompatibility and tissue ingrowth into the hydrogels were histologically examined 4 weeks after implantation. As shown previously in our experiments, this time interval is sufficient for tissue ingrowth into an implanted hydrogel.³⁰

All the hydrogel implants were found to be well-integrated into the surrounding tissue; they closely adhered to the surrounding tissue and formed a bridge across the lesion. Hematoxylin-eosin staining (Fig. 5) as well as cell nuclei (DAPI) staining [Fig. 6(D-F)] showed that the hydrogel pores were entirely filled with the infiltrated cells with no marked differences in tissue infiltration among hydrogels containing 2, 4, or 8 wt % of MOEAA. A sparse foreign body reaction with foamy macrophages [Fig. 5(D,F)] and giant

cell granulomas [Fig. 5(B,D,F)] was found locally around the implanted hydrogels; nevertheless, no adverse reaction with chronic inflammation or fibrosis was detected.

A non-specific inflammatory response with the invasion of macrophages and the formation of multinucleated foreign body giant cells is the reaction of biological tissue to foreign material in the tissue, and the extent of this reaction determines the implant's biocompatibility. Biocompatibility relies basically on surface phenomena, represented by cell-polymer and polymer-protein interactions.⁴² It has been reported that the non-specific adsorption of blood and tissue fluid proteins on the implant surfaces is primarily responsible for phagocyte adsorption and their reaction on implant surfaces.⁴³ The progression of the foreign body reaction is regulated by soluble mediators, such as cytokines, chemokines, and matrix metalloproteinases, which are produced locally by tissue cells and infiltrating inflammatory cells.⁴⁴ Methacrylic polymers, such as PHEMA, are resistant to biodegradation and thus susceptible to cell encapsulation;⁴² nevertheless, PHEMA hydrogels are reported to be well tolerated, non-toxic, and biocompatible. A low occurrence of multinucleated foreign body giant cells was observed on the surface of ocular implants 6 months after implantation.⁴⁵ Modest cellular inflammatory responses that disappeared by 4 weeks postimplantation were observed when PHEMA scaffolds were implanted into cervical spinal cord hemisections.²³ On the other hand, the presence of a fibrous capsule and some foreign-body-type giant cells was reported using 2-hydroxyethyl methacrylate-co-methyl methacrylate)-based nerve guidance channels in the sciatic nerve over a period of 16 weeks.⁴⁶ As shown in Figure 5(B,F), the reaction of foreign body giant cells to superporous cholesterol-modified PHEMA hydrogels was mainly found at the tissue-hydrogel interface, where the difference in mechanical properties between implant and tissue might trigger the encapsulation of the implant. The other reason for the foreign body reaction might be the presence of some hydrogel debris generated during hydrogel shaping and delivered into the tissue during implantation. A significant foreign body reaction was found in our previous study when PHEMA hydrogels with a positive charge were implanted inside the hemisected spinal cord.³⁰ Six months after hydrogel implantation, observation revealed that the granulomatous reaction was significantly reduced with only a minimal or no giant cell reaction, indicating that this type of inflammatory response to the implant diminished over time and did not have any negative effect on the stability of the hydrogels. Nevertheless, for proper determination of the hydrogels' biocompatibility, a longer-term and more detailed analysis of the immune reaction is essential.

In all three hydrogels, NF immunostaining revealed the ingrowth of NF-positive fibers (NF 160 and NF 200 staining) into the pores throughout the whole implant [Fig. 6(A-C)]. The NF-positive fibers were arranged mostly in bundles and originated from the surrounding gray or white matter from the rostral as well as the caudal parts of the surrounding spinal cord and also from the spinal root entry zone.

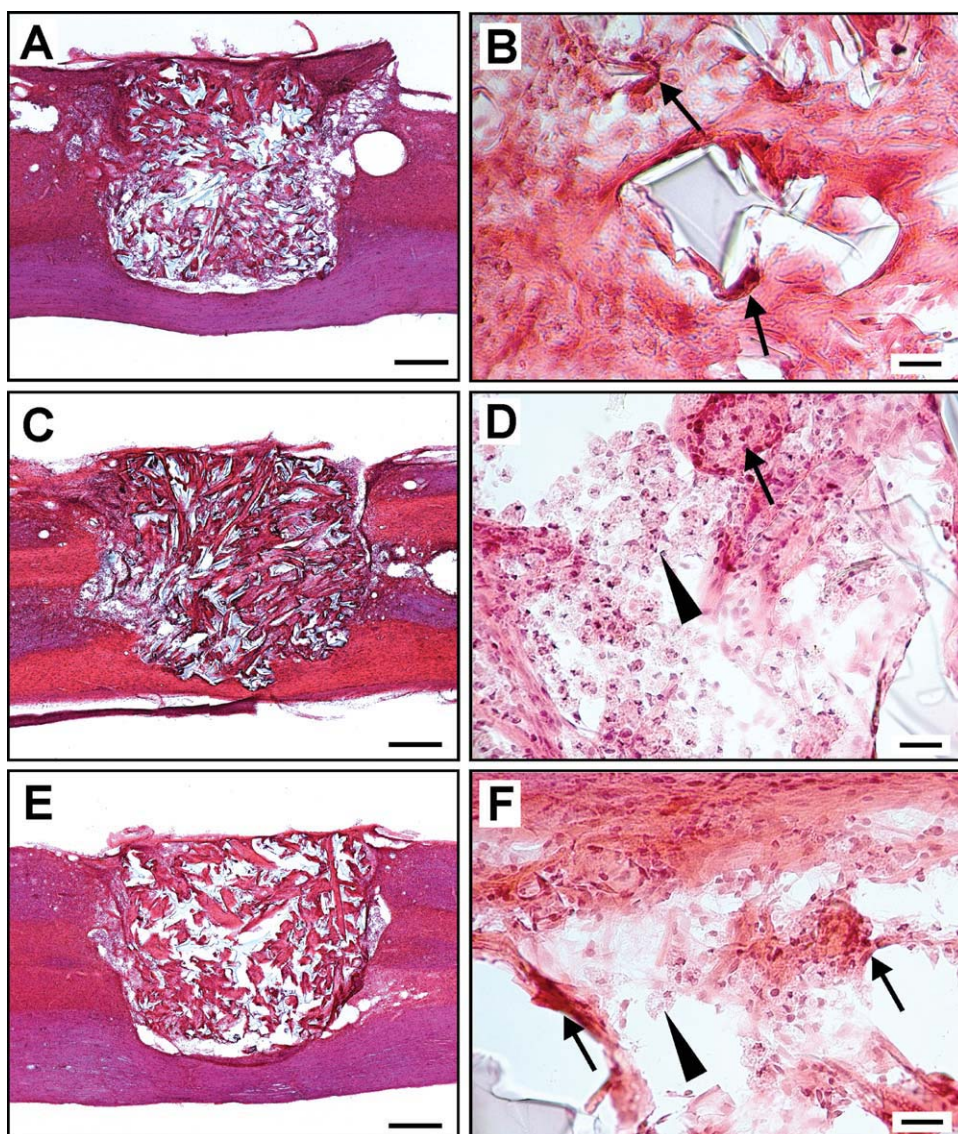


FIGURE 5. H&E staining of spinal cord longitudinal sections with implanted highly superporous (A, B) P(HEMA-2%MOEAA-CHLMA), (C, D) P(HEMA-4%MOEAA-4%AOEEMA-CHLMA), and (E, F) P(HEMA-8%MOEAA-CHLMA) hydrogels. (B, D, F) Foreign body giant cells (arrows) and the (D, F) resorption reaction of macrophages with a foamy cytoplasm (arrowheads) are shown on the right micrographs. Scale bar: (A, C, E) 500 μm and (B, D, F) 10 μm . [Color figure can be viewed in the online issue, which is available at wileyonlinelibrary.com.]

The quantitative evaluation of the area fraction (%) of neurofilament infiltration in the implanted hydrogels did not show any significant differences between the hydrogels containing 2, 4, or 8 wt % of MOEAA (Table II). All of the NF-positive fibers were co-localized with Schwann cells (p75 staining) that infiltrated the hydrogel implants from the spinal root entry zone and provided axon guiding and myelinization (Fig. 7). This is in accordance with many other studies that have demonstrated the beneficial role of Schwann cells for nerve regeneration in the CNS.⁴⁷ However, we cannot exclude the possibility that all of the infiltrating axons might be of peripheral origin. More specific staining of the CNS neuronal tracts needs to be performed to determine the true origin of the regenerating fibers.

Immunostaining against endothelial cells (RECA staining) showed a number of blood vessels that infiltrated the pores throughout the whole hydrogel implant [Fig. 6(D-F)].

No migration of astrocytes or astrocytic process (GFAP staining) ingrowth into the hydrogels was observed [Fig. 6(G-I)]. Similar results have also been reported in other studies of hydrogel spinal cord implants.^{12,30} One month after the implantation of positively and negatively charged PHEMA hydrogels into a spinal cord hemisection, no astrocytic ingrowth was found in the positively charged PHEMA hydrogels, while astrocytes infiltrated the peripheral zone of negatively charged or uncharged hydrogels. On the other hand, positively charged hydrogels showed increased axonal ingrowth into the implant.³⁰ Conversely, the infiltration of

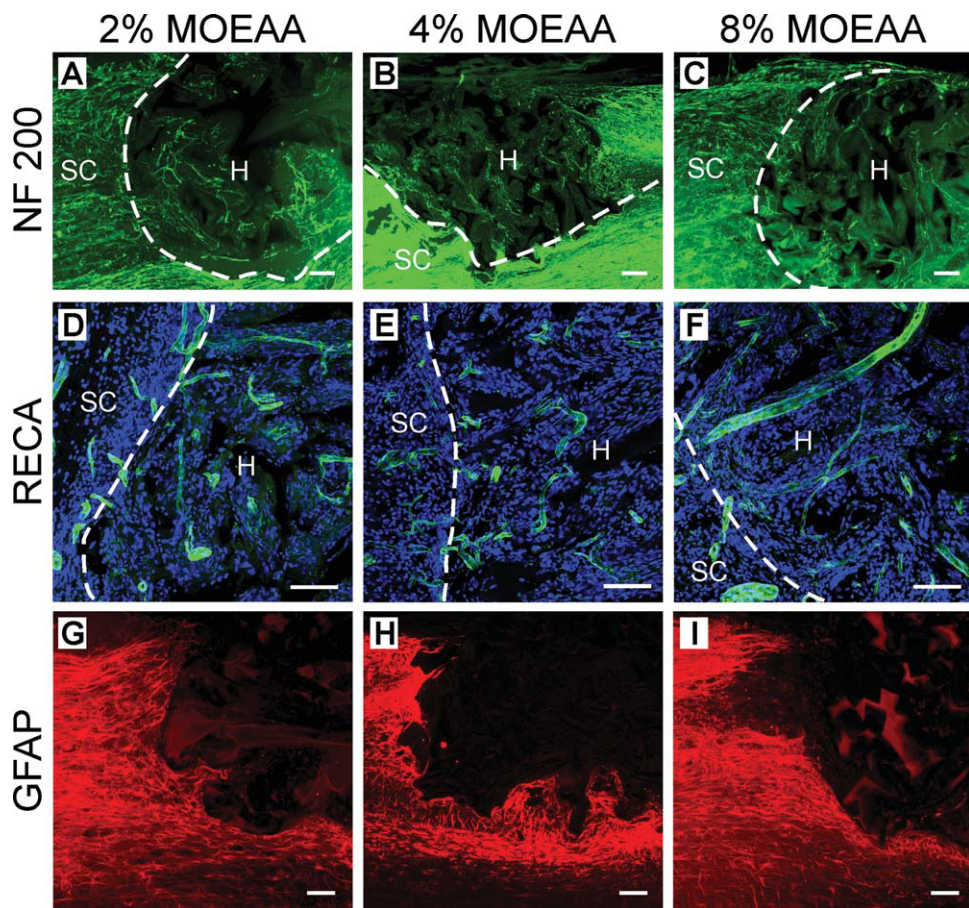


FIGURE 6. Longitudinal spinal cord sections of implanted highly superporous (A, D, G) P(HEMA-2%MOEAA-CHLMA), (B, E, H) P(HEMA-4%MOEAA-4%AOEEMA-CHLMA), and (C, F, I) P(HEMA-8%MOEAA-CHLMA) hydrogels stained for (A–C) neurofilaments (NF160 staining), (D–F) blood vessels (RECA staining) and cell nuclei (DAPI staining), and (G–I) astrocytes (GFAP staining). Dashed lines (A–F) mark the border of the implanted hydrogel (H) in the spinal cord tissue (SC). Scale bar: (A–C) 100 μ m, (D–F) 50 μ m, and (G–I) 100 μ m. [Color figure can be viewed in the online issue, which is available at wileyonlinelibrary.com.]

astrocytes into the peripheral as well as the central parts of PHPMA-RGD hydrogels seeded with MSCs was observed 6 months after implantation, together with an ingrowth of neuronal processes, Schwann cells, and blood vessels.³⁷

The dependence of cell behavior on substrate stiffness has been shown in several studies,^{34,40} but the optimal and/or limiting mechanical properties of the scaffold have not yet been defined in *in vivo* spinal cord experiments. Bakshi et al. (2004) reported that a PHEMA matrix with a compressive modulus of 3–4 kPa matched the spinal cord tissue when implanted into a cervical hemisection.²³ According to our results, the hydrogel compliance, measured as an elastic modulus by compressive testing, ranged

between 10 and 19 kPa. Interestingly, marked differences in the tissue response to hydrogels of such elastic modulus were not found when the hydrogels were transplanted into a hemisection cavity.

SCI comprises a cascade of cellular and biochemical events that lead to the loss of function due to structural damage, glial scarring, and the absence of axonal regeneration. To deal with the complexity of SCI, it is generally assumed that more effective and successful treatment of SCI requires combinatorial strategies involving the application of biomaterials together with cell transplantation and/or the delivery of bioactive molecules, genetic engineering as well as rehabilitation.⁴⁷ In this study, the *in vitro* and *in vivo* biocompatibility of highly superporous cholesterol-modified PHEMA hydrogels was tested and it was shown that these materials can be used to bridge a spinal cord lesion when implanted into a hemisection cavity. However, a more relevant model, such as chronic SCI induced by a balloon compression lesion, should be used for further assessment of this material and its suitability for spinal cord repair. Moreover, to improve the regenerative potential of these hydrogels, combining hydrogels with transplanted cells and/or

TABLE II. Area Fraction (%) of Infiltrated Neurofilaments Inside the Hydrogel

| | | |
|--------------------------------|-----------------|----------|
| P(HEMA-2%MOEAA-CHLMA) | 2.96 ± 1.59 | $n = 14$ |
| P(HEMA-4%MOEAA-4%AOEEMA-CHLMA) | 2.74 ± 1.31 | $n = 22$ |
| P(HEMA-8%MOEAA-CHLMA) | 3.79 ± 2.81 | $n = 11$ |

n, number of evaluated histological slides.

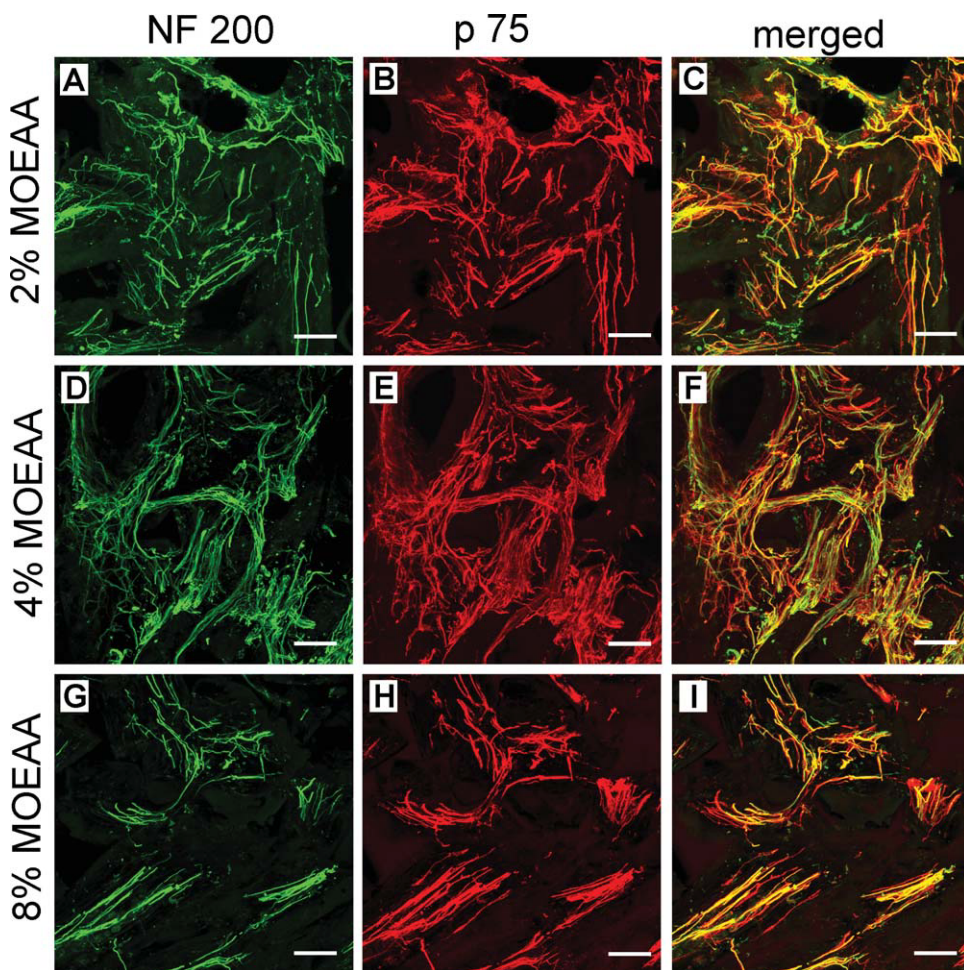


FIGURE 7. Confocal micrographs of the central part of highly superporous (A–C) P(HEMA-2%MOEAA-CHLMA), (D–F) P(HEMA-4%MOEAA-4%AOEEMA-CHLMA), and (G–I) P(HEMA-8%MOEAA-CHLMA) hydrogels 4 weeks after implantation. Immunofluorescent staining for (A, D, G) neurofilaments (NF200) and (B, E, H) Schwann cells (p75). (C, F, I) show the merged micrographs. Scale bar: 20 μ m. [Color figure can be viewed in the online issue, which is available at wileyonlinelibrary.com.]

growth factors, as well as further evaluations such as functional assessment involving behavioral testing or axonal tracing, need to be performed.

CONCLUSIONS

Cholesterol-modified superporous PHEMA scaffolds have been prepared by the bulk radical copolymerization of HEMA, CHLMA, and the crosslinking agent EDMA. The modification of PHEMA with cholesterol has been employed to improve cell adhesion and the proper integration of the biomaterial after implantation. To increase swellability, MCMEMA was incorporated in the polymerization recipe and hydrolyzed to MOEAA, thus introducing carboxyl groups in the polymer. Three types of PHEMA hydrogels containing 2, 4, or 8 wt % of MOEAA were prepared, differing in both swelling and surface charge. The repeated loading of ammonium oxalate crystals induced high porosity (65 vol %) and the formation of interconnected pores 30–100 μ m in size, which is desirable for the ingrowth of stem cells into the pores of the scaffold for SCI repair. According to the elastic modulus, hydrogel compliance decreased in the order

P(HEMA-8%MOEAA-CHLMA), P(HEMA-2%MOEAA-CHLMA), and P(HEMA-4%MOEAA-4%AOEEMA-CHLMA). In cell culture, highly superporous cholesterol-modified hydrogels supported the adhesion and growth of MSCs. After transplantation into a hemisected spinal cord, the hydrogels formed bridge across the lesion and promoted axonal and Schwann cell infiltration and angiogenesis inside the hydrogel pores. No differences in hydrogel integration into the hemisection cavity or in tissue infiltration were observed between the hydrogels containing 2, 4, or 8 wt % of MOEAA.

In conclusion, all types of highly superporous cholesterol-modified PHEMA hydrogels can be used as scaffolds in SCI repair. Nevertheless, additional treatment strategies incorporating aligned pore orientation and/or cell transplantation should be implemented to support the regenerative potential of hydrogel scaffolds.

REFERENCES

- Raineteau O. Plastic responses to spinal cord injury. *Behav Brain Res* 2008;192:114–123.

2. Fitch MT, Silver J. CNS injury, glial scars, and inflammation: Inhibitory extracellular matrices and regeneration failure. *Exp Neurol* 2008;209:294–301.
3. Willerth SM, Sakiyama-Elbert SE. Cell therapy for spinal cord regeneration. *Adv Drug Deliv Rev* 2008;60:263–276.
4. Sykova E, Jendelova P. Migration, fate and *in vivo* imaging of adult stem cells in the CNS. *Cell Death Differ* 2007;14:1336–1342.
5. Straley KS, Foo CW, Heilshorn SC. Biomaterial design strategies for the treatment of spinal cord injuries. *J Neurotrauma* 2010;27:1–19.
6. Nisbet DR, Crompton KE, Horne MK, Finkelstein DL, Forsythe JS. Neural tissue engineering of the CNS using hydrogels. *J Biomed Mater Res B* 2008;87:251–263.
7. Tysseling-Mattiace VM, Sahni V, Niece KL, Birch D, Czeisler C, Fehlings MG, Stupp SI, Kessler JA. Self-assembling nanofibers inhibit glial scar formation and promote axon elongation after spinal cord injury. *J Neurosci* 2008;28:3814–3823.
8. Guo J, Su H, Zeng Y, Liang YX, Wong WM, Ellis-Behnke RG, So KF, Wu W. Reknitting the injured spinal cord by self-assembling peptide nanofiber scaffold. *Nanomedicine* 2007;3:311–321.
9. Gelain F, Panseri S, Antonini S, Cunha C, Donega M, Lowery J, Taraballi F, Cerri G, Montagna M, Baldissera F, Vescovi A. Transplantation of nanostructured composite scaffolds results in the regeneration of chronically injured spinal cords. *ACS Nano* 2011;5:227–236.
10. Tsai EC, Dalton PD, Shoichet MS, Tator CH. Matrix inclusion within synthetic hydrogel guidance channels improves specific supraspinal and local axonal regeneration after complete spinal cord transection. *Biomaterials* 2006;27:519–533.
11. Nomura H, Tator CH, Shoichet MS. Bioengineered strategies for spinal cord repair. *J Neurotrauma* 2006;23:496–507.
12. Novikova LN, Pettersson J, Brohlin M, Wiberg M, Novikov LN. Biodegradable poly-beta-hydroxybutyrate scaffold seeded with Schwann cells to promote spinal cord repair. *Biomaterials* 2008;29:1198–1206.
13. Madaghie M, Sannino A, Yannas IV, Spector M. Collagen-based matrices with axially oriented pores. *J Biomed Mater Res A* 2008;85:757–767.
14. Prang P, Muller R, Eljaouhari A, Heckmann K, Kunz W, Weber T, Faber C, Vroemen M, Bogdahn U, Weidner N. The promotion of oriented axonal regrowth in the injured spinal cord by alginate-based anisotropic capillary hydrogels. *Biomaterials* 2006;27:3560–3569.
15. Wei YT, He Y, Xu CL, Wang Y, Liu BF, Wang XM, Sun XD, Cui FZ, Xu QY. Hyaluronic acid hydrogel modified with nog-66 receptor antibody and poly-L-lysine to promote axon regrowth after spinal cord injury. *J Biomed Mater Res B* 2010;95:110–117.
16. Park J, Lim E, Back S, Na H, Park Y, Sun K. Nerve regeneration following spinal cord injury using matrix metalloproteinase-sensitive, hyaluronic acid-based biomimetic hydrogel scaffold containing brain-derived neurotrophic factor. *J Biomed Mater Res A* 2010;93:1091–1099.
17. Gros T, Sakamoto JS, Blesch A, Hayton LA, Tuszyński MH. Regeneration of long-tract axons through sites of spinal cord injury using templated agarose scaffolds. *Biomaterials* 2010;31:6719–6729.
18. Taylor SJ, Rosenzweig ES, McDonald JW III, Sakiyama-Elbert SE. Delivery of neurotrophin-3 from fibrin enhances neuronal fiber sprouting after spinal cord injury. *J Control Release* 2006;113:226–235.
19. Madigan NN, McMahon S, O'Brien T, Yaszemski MJ, Windebank AJ. Current tissue engineering and novel therapeutic approaches to axonal regeneration following spinal cord injury using polymer scaffolds. *Respir Physiol Neurobiol* 2009;169:183–199.
20. Zhu J. Bioactive modification of poly(ethylene glycol) hydrogels for tissue engineering. *Biomaterials* 2010;31:4639–4656.
21. Tsai EC, Dalton PD, Shoichet MS, Tator CH. Synthetic hydrogel guidance channels facilitate regeneration of adult rat brainstem motor axons after complete spinal cord transection. *J Neurotrauma* 2004;21:789–804.
22. Hejcl A, Lesny P, Pradny M, Michalek J, Jendelova P, Stulik J, Sykova E. Biocompatible hydrogels in spinal cord injury repair. *Physiol Res* 2008;57 (Suppl 3):S121–S132.
23. Bakshi A, Fisher O, Dagci T, Himes BT, Fischer I, Lowman A. Mechanically engineered hydrogel scaffolds for axonal growth and angiogenesis after transplantation in spinal cord injury. *J Neurosurg Spine* 2004;1:322–329.
24. Woerly S, Fort S, Pignot-Paintrand I, Cottet C, Carcenac C, Savasta M. Development of a sialic acid-containing hydrogel of poly[N-(2-hydroxypropyl) methacrylamide]: Characterization and implantation study. *Biomacromolecules* 2008;9:2329–2337.
25. Olson HE, Rooney GE, Gross L, Nesbitt JJ, Galvin KE, Knight A, Chen B, Yaszemski MJ, Windebank AJ. Neural stem cell- and Schwann cell-loaded biodegradable polymer scaffolds support axonal regeneration in the transected spinal cord. *Tissue Eng Part A* 2009;15:1797–1805.
26. Lee H, McKeon RJ, Bellamkonda RV. Sustained delivery of thermosabilized chABC enhances axonal sprouting and functional recovery after spinal cord injury. *Proc Natl Acad Sci USA* 2010;107:3340–3345.
27. Katz JS, Burdick JA. Hydrogel mediated delivery of trophic factors for neural repair. *Wiley Interdiscip Rev Nanomed Nanobiotechnol* 2009;1:128–139.
28. Baumann MD, Kang CE, Tator CH, Shoichet MS. Intrathecal delivery of a polymeric nanocomposite hydrogel after spinal cord injury. *Biomaterials* 2010;31:7631–7639.
29. Horák D, Jayakrishnan A, Arshady R. Poly(2-hydroxyethyl methacrylate) Hydrogels. Preparation and Properties. London: Citus Books 2003. p 65–107.
30. Hejcl A, Lesny P, Pradny M, Sedy J, Zamecnik J, Jendelova P, Michalek J, Sykova E. Macroporous hydrogels based on 2-hydroxyethyl methacrylate. Part 6: 3D hydrogels with positive and negative surface charges and polyelectrolyte complexes in spinal cord injury repair. *J Mater Sci Mater Med* 2009;20:1571–1577.
31. Kubinova S, Horak D, Kozubenko N, Vanecik V, Proks V, Price J, Cocks G, Sykova E. The use of superporous Ac-CGGASIKVAVS-OH-modified PHEMA scaffolds to promote cell adhesion and the differentiation of human fetal neural precursors. *Biomaterials* 2010;31:5966–5975.
32. Yu TT, Shoichet MS. Guided cell adhesion and outgrowth in peptide-modified channels for neural tissue engineering. *Biomaterials* 2005;26:1507–1514.
33. Kubinova S, Horak D, Sykova E. Cholesterol-modified superporous poly(2-hydroxyethyl methacrylate) scaffolds for tissue engineering. *Biomaterials* 2009;30:4601–4609.
34. Engler AJ, Sen S, Sweeney HL, Discher DE. Matrix elasticity directs stem cell lineage specification. *Cell* 2006;126:677–689.
35. Ozawa H, Matsumoto T, Ohashi T, Sato M, Kokubun S. Comparison of spinal cord gray matter and white matter softness: measurement by pipette aspiration method. *J Neurosurg* 2001;95:221–224.
36. Salem HK, Thiemermann C. Mesenchymal stromal cells: Current understanding and clinical status. *Stem Cells* 2010;28:585–596.
37. Hejcl A, Sedy J, Kapcalova M, Toro DA, Amemori T, Lesny P, Likavcanova-Masinova K, Krumbholcova E, Pradny M, Michalek J, Burian M, Hajek M, Jendelova P, Sykova E. HPMA-RGD hydrogels seeded with mesenchymal stem cells improve functional outcome in chronic spinal cord injury. *Stem Cells Dev* 2010;19:1535–1546.
38. Lesny P, Pradny M, Jendelova P, Michalek J, Vacik J, Sykova E. Macroporous hydrogels based on 2-hydroxyethyl methacrylate. Part 4: growth of rat bone marrow stromal cells in three-dimensional hydrogels with positive and negative surface charges and in polyelectrolyte complexes. *J Mater Sci Mater Med* 2006;17:829–833.
39. Lesny P, De Croos J, Pradny M, Vacik J, Michalek J, Woerly S, Sykova E. Polymer hydrogels usable for nervous tissue repair. *J Chem Neuroanat* 2002;23:243–247.
40. Leach JB, Brown XQ, Jacot JG, Dimilla PA, Wong JY. Neurite outgrowth and branching of PC12 cells on very soft substrates sharply decreases below a threshold of substrate rigidity. *J Neural Eng* 2007;4:26–34.
41. Babaeijandaghi F, Shabani I, Seyedjafari E, Naraghi ZS, Vasei M, Haddadi-Asl V, Hesari KK, Soleimani M. Accelerated epidermal regeneration and improved dermal reconstruction achieved by polyethersulfone nanofibers. *Tissue Eng Part A* 2011;16:3527–3536.

42. Fournier E, Passirani C, Montero-Menei CN, Benoit JP. Biocompatibility of implantable synthetic polymeric drug carriers: Focus on brain biocompatibility. *Biomaterials* 2003;24: 3311–3331.
43. Hu WJ, Eaton JW, Ugarova TP, Tang L. Molecular basis of biomaterial-mediated foreign body reactions. *Blood* 2001;98: 1231–1238.
44. Luttkhuizen DT, Harmsen MC, Van Luyn MJ. Cellular and molecular dynamics in the foreign body reaction. *Tissue Eng* 2006;12: 1955–1970.
45. Smetana K Jr, Sulc J, Krcova Z, Pitrova S. Intraocular biocompatibility of hydroxyethyl methacrylate and methacrylic acid copolymer/partially hydrolyzed poly(2-hydroxyethyl methacrylate). *J Biomed Mater Res* 1987;21:1247–1253.
46. Belkas JS, Munro CA, Shoichet MS, Johnston M, Midha R. Long-term *in vivo* biomechanical properties and biocompatibility of poly(2-hydroxyethyl methacrylate-co-methyl methacrylate) nerve conduits. *Biomaterials* 2005;26:1741–1749.
47. Bunge MB. Novel combination strategies to repair the injured mammalian spinal cord. *J Spinal Cord Med* 2008;31:262–269.